Mohammed and Al-Muslimawi Iraqi Journal of Science, 2023, Vol. 64, No. 3, pp: 1331-1343
DOI: 10.24996/ijs.2023.64.3.27

ISSN: 0067-2904

# Numerical Study of Compressible and Weak Compressible Flows in Channel Based on Artificial Compressibility Method and Fully Artificial Compressibility Method

**Fatima A.Mohammed*, Alaa H. Al-Muslimawi**
*Department of Mathematics, College of Science, University of Basrah, Basrah, Iraq*

Received: 28/2/2022 Accepted: 20/7/2022 Published: 30/3/2023

**Abstract**

In this article, a numerical study of compressible and weak compressible Newtonian flows is achieved for a time marching, Galerkin algorithm. A comparison between two numerical techniques for such flows, namely the artificial compressibility method (AC–method) and the fully artificial compressibility method (FAC–method) is performed. In the first artificial compressibility parameter ($C^2$) is added to the continuity equation, while this parameter is added to both continuity and momentum equations in the second technique. This strategy is implemented to treat the governing equations of Newtonian flow in cylindrical coordinates (axisymmetric). Particularly, this study concerns with the effect of the artificial compressibility parameters on the convergence level of solutions components. To confirm the analysis of these approaches, Poiseuille flow along a circular channel under an isothermal state is used as a simple test problem. The results show that when the AC-method is used there is a significant reduction in the level of time convergence of pressure and axial velocity compared to that with FAC-method. Here, for compressible flow the Tail model of state is employed to relate the pressure to density. In this context, the effect of Tail parameters and Reynolds number on the time convergence of solution components is also investigated in the present study. The results indicate a significant reduction in the time-stepping convergence as increasing in the {B,m}-value. In contrast, more difficulties are faced in the convergence when the level of the Reynolds number is increasing.

**Keywords**: Artificial Compressibility Method, Compressible Fluid Flow, FullyArtificial Compressibility Method ,Newtonian Fluids, Numerical Methods.

# دراسة عددية لجريانات السوائل القابلة للانضغاط وضعيفة الانضغاطية في قناة بناءً على طريقة الانضغاط الاصطناعي وطريقة الانضغاط الاصطناعي الكامل

**فاطمة عبد الرزاق محمد* ، علاء حسن المسلماوي**
قسم الرياضيات، كلية العلوم، جامعة البصرة، البصرة، العراق

**الخلاصة**

في هذه البحث، تم إجراء دراسة عددية لجريانات السوائل النيوتونية القابلة للانضغاط والضعيفة القابلية للانضغاطية في اثناء جريانها في فترة زمنية محددة، باستخدام خوارزمية كالركين(Galerkin). تم اجراء مقارنة بين

* Email: fatimaalmazini@gmail.com

تطبيق طريقتين رقميتين لدراسة مثل هذه الجريانات؛ حيث تم تطبيق طريقة الانضغاط الاصطناعي (طريقة AC ) وطريقة الانضغاط الاصطناعي الكامل (طريقة FAC). في الطريقة الاولى يضاف معامل انضغاط اصطناعي ($C^2$) إلى معادلة الاستمرارية فقط، بينما يضاف هذا المعامل إلى معادلات الاستمرارية والزخم في الطريقة الثانية. تم تطبيق هذه الاستراتيجية لمعالجة المعادلات الحاكمة لجريان السوائل النيوتونية في إحداثيات أسطوانية (محور متماثل). تهتم هذه الدراسة بشكل خاص بدراسة تأثير معلمات الانضغاط الاصطناعي على مستوى تقارب مكونات الحل. للتأكيد من تحليل هذه الطرق، يتم استخدام جريان برنولي (Poiseuille) على طول قناة دائرية تحت ظروف حرارية متجانسة كمسألة بسيطة يتم اختبارها. أظهرت النتائج ان استخدام طريقة الانضغاط الاصطناعي (طريقة AC) يحدث انخفاض كبير في مستوى تقارب الوقت للضغط والسرعة المحورية مقارنة مع طريقة الانضغاط الاصطناعي بالكامل (طريقة FAC). بالنسبة لجريان السوائل القابلة للانضغاط، تم استخدام نموذج تايل ( Tail model) للحالة لربط الضغط بالكثافة. في هذا السياق ، تم أيضًا دراسة تأثير معلمات تايل ورقم رينولدز على تقارب الوقت لمكونات الحل. تشير النتائج أيضا إلى انخفاض كبير في تقارب الوقت مع زيادة في قيمة {m,B}(معلمات تايل) في المقابل ، يتم مواجهة المزيد من الصعوبة في التقارب عندما تزداد قيمة رقم رينولدز.

## 1. Introduction

Compressible flow techniques have been obtained more attention due to the various and useful applications in the practical fields. However, over the latest years, the involvement of complicated geometries leads to an increase in the demand for flow simulation products. The artificial compressibility method (AC -method) was originally introduced by Chorin (1967) with the objective of solving Navier-Stokes equations, the pressure components can be computed both inside and at the boundaries of the domain when the velocity is given [1]. This method was presented as one of many approaches that were planned for acclimating computational grids to complex geometries by unstructured meshes [2]. The use of AC method gives extra facilities. These facilities helped to overcome such problems as extra terms in the equations, extra insinuation, larger computational molecules and problems associated with the transfer of information across grid interfaces. The main idea of this method is to add a fictitious time derivative of pressure to the continuity to transform the system of equations from an elliptic incompressible system to a hyperbolic compressible system [2,3]. In this technique, there is an artificial continuity equation with the pressure time derivative [4]. A new transformed equation will be formed, but this equation can be directly solved by the standard time-dependent approach that is not complicated to apply to the solution, so the solution is obtained much quicker than other primitive variable methods that require the solution of another derived equation at each time step. The addition of the artificial compressibility term will be disappeared when the steady state solution is reached [5]. In his study, Chorin introduced his method in order to solve the steady state incompressible Navier-Stokes differential equations, while other researchers tried to extend this method to include unsteady state such as Peyret and Taylor [6] and Kao and Yang [7]. Annually, there are many studies that discuss the applications of using the artificial compressibility method. Its applications are almost limited to solve the velocity-pressure formulation for incompressible fluids. The novelty in the present study is to add an artificial term derivative to both continuity and momentum equations of compressible fluids as fully artificial compressibility (FAC), which has not been addressed before. The present study aims to provide a study for compressible Newtonian fluid flows by finite element method dependent on simple shear-rate. In this context, Poiseuille (Ps) flow along a two dimensional planar straight channel under isothermal conditions is studied. The main results of the current study are focused on making a comparison between the effect of the use of fully artificial compressibility beside artificial compressibility on the convergence of pressure and velocity components. Numerical treatments are presented for the governing system, where we have utilized the Galerkin finite element method based on AC-method and FAC-method, which has also not been addressed before. For the numerical solution, the iterative method of Newton-Raphson will be used to solve the set of non-linear equations and the backward different scheme will be employed as the time-integration approach to deal with the time dependent term.

## 2. Mathematical modeling

The dimensionless form of continuity and momentum equations of compressible Newtonian flow under the isothermal conditions with omitting the body forces can be given in cylindrical coordinates as follows [8,9]:

$$\frac{\partial \rho}{\partial t}+\frac{1}{r}\frac{\partial}{\partial r}(\rho r u_r)+\frac{1}{r}\frac{\partial}{\partial \theta}(\rho u_\theta)+\frac{\partial}{\partial z}(\rho u_z)=0. \tag{1}$$

**The r-direction**

$$\rho\left(\frac{\partial U_r}{\partial t}+U_r\frac{\partial U_r}{\partial r}+\frac{U_\theta}{r}\frac{\partial U_r}{\partial \theta}+U_z\frac{\partial U_r}{\partial z}-\frac{U_\theta U_\theta}{r}\right)$$
$$=-\frac{\partial p}{\partial r}+\frac{4\mu}{3}\frac{\partial^2 U_r}{\partial r^2}+\frac{4\mu}{3r}\frac{\partial U_r}{\partial r}-\frac{4\mu}{3r^2}U_r+\frac{\mu}{3r}\frac{\partial^2 U_\theta}{\partial r\partial \theta}-\frac{4\mu}{3r^2}\frac{\partial U_\theta}{\partial \theta}$$
$$+\frac{\mu}{r^2}\frac{\partial^2 U_r}{\partial \theta^2}+\mu\frac{\partial^2 U_r}{\partial z^2}+\frac{\mu}{3}\frac{\partial^2 U_z}{\partial r\partial z}-\frac{\mu}{r^2}\frac{\partial U_r}{\partial r} \tag{2}$$

**The $\boldsymbol{\theta}$-direction**

$$\rho\left(\frac{\partial U_\theta}{\partial t}+U_r\frac{\partial U_\theta}{\partial r}+\frac{U_\theta}{r}\frac{\partial U_\theta}{\partial \theta}+U_z\frac{\partial U_\theta}{\partial z}+\frac{\partial U_r U_\theta}{r}\right)$$
$$=-\frac{1}{r}\frac{\partial p}{\partial \theta}+\frac{\mu}{3r}\frac{\partial^2 U_r}{\partial r\partial \theta}+\frac{7\mu}{3r^2}\frac{\partial U_r}{\partial \theta}+\frac{4\mu}{3r^2}\frac{\partial^2 U_\theta}{\partial \theta^2}$$
$$+\frac{\mu}{3r}\frac{\partial^2 U_z}{\partial \theta\partial z}+\mu\frac{\partial^2 u_\theta}{\partial z^2}+\mu\frac{\partial^2 u_\theta}{\partial r^2}+\frac{\mu}{r}\frac{\partial U_\theta}{\partial r}-\frac{\mu}{r^2}U_\theta \tag{3}$$

**The z-direction**

$$\rho\left(\frac{\partial U_z}{\partial t}+U_r\frac{\partial U_z}{\partial r}+\frac{U_\theta}{r}\frac{\partial U_z}{\partial \theta}+U_z\frac{\partial U_z}{\partial z}\right)$$
$$=-\frac{\partial p}{\partial z}-\frac{2\mu}{3}\frac{\partial^2 U_r}{\partial r\partial z}+\frac{\mu}{3r}\frac{\partial U_r}{\partial z}+\frac{\mu}{3r}\frac{\partial^2 U_\theta}{\partial \theta\partial z}+\frac{4\mu}{3}\frac{\partial^2 U_z}{\partial z^2}$$
$$+\mu\frac{\partial^2 U_z}{\partial r^2}+\mu\frac{\partial^2 U_z}{\partial r\partial z}+\frac{\mu}{r^2}\frac{\partial^2 U_z}{\partial \theta^2}+\frac{\mu}{r}\frac{\partial U_z}{\partial r} \tag{4}$$

Where $u_r, u_\theta$ and $u_z$ are the velocity components in $r$-direction, the $\theta$-direction and the $z$-direction, respectively, $p$ is the pressure and $\rho$ is the fluid density ,for more details see [8].

## 3. AC-method and FAC-method

**AC-mathod:** In this technique, the incompressible elliptic differential equation is transformed into the hyperbolic compressible partial differential by adding the artificial term into the continuity equation. The addition of the artificial compressibility term will vanish when the steady state solution is reached [21,23]. For more detials on applying this method, see [8].

**FAC-mathod:** In order to describe this method, let us apply the artificial term into continuity and momentum equations. Here, the artificial density is related to the pressure by the artificial Tait equation of state [22].

$$\mathrm{P}=c^2 \tag{5}$$

So that

$$\rho=\frac{1}{c^2}p \tag{6}$$

Where as

$$c^2 = \mathrm{m(p + B)} \tag{7}$$

where $(C^2)$ is the artificial compressibility parameter such that $0 < \frac{1}{c^2} < 1$. By substituting equation (6) into equations 1,2,3 and 4, we get the new form of fully artificial compressibility continuity and momentum equations as follows:

$$\frac{1}{c^2}\frac{\partial p}{\partial t} + \frac{1}{c^2}p\frac{\partial U_r}{\partial r} + u_r\frac{\partial \rho}{\partial r} + \frac{1}{c^2}\frac{p}{r}u_r + \frac{1}{c^2}\frac{p}{r}\frac{\partial U_\theta}{\partial \theta} + \frac{U_\theta}{r}\frac{\partial \rho}{\partial \theta} + \frac{1}{c^2}\mathrm{p}\frac{\partial U_z}{\partial z} + U_z\frac{\partial \rho}{\partial z} = 0 \tag{8}$$

**The r-direction**

$$\frac{1}{c^2}\boldsymbol{p}\left(\frac{\partial U_r}{\partial t} + U_r\frac{\partial U_r}{\partial r} + \frac{U_\theta}{r}\frac{\partial U_r}{\partial \theta} + U_z\frac{\partial U_r}{\partial z} - \frac{U_\theta U_\theta}{r}\right)$$

$$= -\frac{\partial \rho}{\partial r} + \frac{4\mu}{3}\frac{\partial^2 U_r}{\partial r^2} + \frac{4\mu}{3r}\frac{\partial U_r}{\partial r} - \frac{4\mu}{3r^2}U_r + \frac{\mu}{3r}\frac{\partial^2 U_\theta}{\partial r\partial \theta} - \frac{4\mu}{3r^2}\frac{\partial U_\theta}{\partial \theta}$$

$$+\frac{\mu}{r^2}\frac{\partial^2 U_r}{\partial \theta^2} + \mu\frac{\partial^2 U_r}{\partial z^2} + \frac{\mu}{3}\frac{\partial^2 U_z}{\partial r\partial z} - \frac{\mu}{r^2}\frac{\partial U_r}{\partial r} \tag{9}$$

**The $\boldsymbol{\theta}$-direction**

$$\frac{1}{c^2}\boldsymbol{p}\left(\frac{\partial U_\theta}{\partial t} + U_r\frac{\partial U_\theta}{\partial r} + \frac{U_\theta}{r}\frac{\partial U_\theta}{\partial \theta} + U_z\frac{\partial U_\theta}{\partial z} + \frac{\partial U_r U_\theta}{r}\right)$$

$$= -\frac{1}{r}\frac{\partial \rho}{\partial \theta} + \frac{\mu}{3r}\frac{\partial^2 U_r}{\partial r\partial \theta} + \frac{7\mu}{3r^2}\frac{\partial U_r}{\partial \theta} + \frac{4\mu}{3r^2}\frac{\partial^2 U_\theta}{\partial \theta^2}$$

$$+\frac{\mu}{3r}\frac{\partial^2 U_z}{\partial \theta\partial z} + \mu\frac{\partial^2 u_\theta}{\partial z^2} + \mu\frac{\partial^2 u_\theta}{\partial r^2} + \frac{\mu}{r}\frac{\partial U_\theta}{\partial r} - \frac{\mu}{r^2}U_\theta \tag{10}$$

**The Z-direction**

$$\frac{1}{c^2}\boldsymbol{p}\left(\frac{\partial U_z}{\partial t} + U_r\frac{\partial U_z}{\partial r} + \frac{U_\theta}{r}\frac{\partial U_z}{\partial \theta} + U_z\frac{\partial U_z}{\partial z}\right)$$

$$= -\frac{\partial \rho}{\partial z} - \frac{2\mu}{3}\frac{\partial^2 U_r}{\partial r\partial z} + \frac{\mu}{3r}\frac{\partial U_r}{\partial z} + \frac{\mu}{3r}\frac{\partial^2 U_\theta}{\partial \theta\partial z} + \frac{4\mu}{3}\frac{\partial^2 U_z}{\partial z^2}$$

$$+\mu\frac{\partial^2 U_z}{\partial r^2} + \mu\frac{\partial^2 U_z}{\partial r\partial z} + \frac{\mu}{r^2}\frac{\partial^2 U_z}{\partial \theta^2} + \frac{\mu}{r}\frac{\partial U_z}{\partial r} \tag{11}$$

Now, the weak form the discretization of (5) is based on artificial compressibility method, it can
be expressed as

$$\int_\Omega q\left(\frac{1}{c^2}\frac{\partial p}{\partial t} + \frac{1}{c^2}p\frac{\partial U_r}{\partial r} + u_r\frac{\partial \rho}{\partial r} + \frac{1}{c^2}\frac{p}{r}u_r + \frac{1}{c^2}\frac{p}{r}\frac{\partial U_\theta}{\partial \theta} + \frac{U_\theta}{r}\frac{\partial \rho}{\partial \theta} + \frac{1}{c^2}p\frac{\partial U_z}{\partial z} + U_z\frac{\partial \rho}{\partial z}\right)\partial\Omega = 0 \tag{12}$$

**r-direction**

$$\int_\Omega \frac{1}{c^2}\boldsymbol{w}\,\boldsymbol{p}\left(\frac{\partial U_r}{\partial t} + U_r\frac{\partial U_r}{\partial r} + \frac{U_\theta}{r}\frac{\partial U_r}{\partial \theta} + U_z\frac{\partial U_r}{\partial z} - \frac{U_\theta U_\theta}{r}\right)\partial\Omega$$

$$= \int_\Omega \frac{W}{Re}\left(-\frac{\partial \rho}{\partial r} + \frac{4\mu}{3}\frac{\partial^2 U_r}{\partial r^2} + \frac{4\mu}{3r}\frac{\partial U_r}{\partial r} - \frac{4\mu}{3r^2}U_r + \frac{\mu}{3r}\frac{\partial^2 U_\theta}{\partial r\partial \theta} - \frac{4\mu}{3r^2}\frac{\partial U_\theta}{\partial \theta}\right.$$

$$+\frac{\mu}{r^2}\frac{\partial^2 U_r}{\partial\theta^2}+\mu\frac{\partial^2 U_r}{\partial z^2}+\frac{\mu}{3}\frac{\partial^2 U_z}{\partial r\partial z}-\frac{\mu}{r^2}\frac{\partial U_r}{\partial r})\partial\Omega=0 \quad (13)$$

**$\theta$-direction**

$$\int_\Omega \frac{1}{c^2}wp(\frac{\partial U_\theta}{\partial t}+U_r\frac{\partial U_\theta}{\partial r}+\frac{U_\theta}{r}\frac{\partial U_\theta}{\partial\theta}+U_z\frac{\partial U_\theta}{\partial z}+\frac{\partial U_r U_\theta}{r})$$
$$=\int_\Omega \frac{W}{Re}(-\frac{1}{r}\frac{\partial\rho}{\partial\theta}+\frac{\mu}{3r}\frac{\partial^2 U_r}{\partial r\partial\theta}+\frac{7\mu}{3r^2}\frac{\partial U_r}{\partial\theta}+\frac{4\mu}{3r^2}\frac{\partial^2 U_\theta}{\partial\theta^2}$$

$$+\frac{\mu}{3r}\frac{\partial^2 U_z}{\partial\theta\partial z}+\mu\frac{\partial^2 u_\theta}{\partial z^2}+\mu\frac{\partial^2 u_\theta}{\partial r^2}+\frac{\mu}{r}\frac{\partial U_\theta}{\partial r}-\frac{\mu}{r^2}U_{\theta)}\partial\Omega=0 \quad (14)$$

**Z-direction**

$$\int_\Omega \frac{1}{c^2}w\,p(\frac{\partial U_z}{\partial t}+U_r\frac{\partial U_z}{\partial r}+\frac{U_\theta}{r}\frac{\partial U_z}{\partial\theta}+U_z\frac{\partial U_z}{\partial z})$$
$$=\int_\Omega \frac{W}{Re}(-\frac{\partial\rho}{\partial z}-\frac{2\mu}{3}\frac{\partial^2 U_r}{\partial r\partial z}+\frac{\mu}{3r}\frac{\partial U_r}{\partial z}+\frac{\mu}{3r}\frac{\partial^2 U_\theta}{\partial\theta\partial z}+\frac{4\mu}{3}\frac{\partial^2 U_z}{\partial z^2}$$
$$+\mu\frac{\partial^2 U_z}{\partial r^2}+\mu\frac{\partial^2 U_z}{\partial r\partial z}+\frac{\mu}{r^2}\frac{\partial^2 U_z}{\partial\theta^2}+\frac{\mu}{r}\frac{\partial U_z}{\partial r})\partial\Omega=0 \quad (15)$$

Thus, from divergence theorem and rearranging the terms, we obtain the weak form of the continuity equation in the case of weak incompressible flow as follows:

$$[M\rho][\rho^\cdot]+[Q_1][U_r]+[q_1][\rho]+[S][U_r]+[Q_2][U_\forall]+[q_2][\rho]+[Q_3][U_z]+[q_3][\rho]=0 \quad (16)$$

$$[M][U_r]+[C_r(U_r)][U_r]+[C_z(U_z)][U_r]-[C_\theta][U_\theta]-\frac{1}{\mathrm{Re}}[Q_r][\rho]+\frac{4}{3}[K_{r_r}][U_r]$$
$$+\frac{4}{3}[K_r][U_r]+\frac{4}{3}[q_r][U_r]+[K_{z_z}][U_r]+\frac{1}{3}[K_{r_z}][U_z]=0 \quad (17)$$

$$[M][U_\theta]+[C_r(U_r)][U_\theta]+[C_z(U_z)][U_\theta]-[C_r][U_\theta]+[K_{z_z}][U_\theta]$$
$$+[K_{r_r}][U_\theta]+[K_r][U_\theta]+[q_\theta][U_\theta]=0 \quad (18)$$

$$[M][U_z]+[C_r(U_r)][U_z]+[C_z(U_z)][U_z]-\frac{1}{Re}[Q_z][\rho]-\frac{2}{3}[K_{rz}][U_r]+\frac{1}{3}[K_z][U_r]+\frac{4}{3}[K_{z_z}][U_z]$$
$$+[K_{r_r}][U_z]+[K_{r_z}][U_z]+[K_r][U_z]=0 \quad (19)$$

$$[M\rho]=\frac{1}{c^2}\int_\Omega \emptyset\emptyset\,\tau\,\partial\Omega$$
$$[M\rho]=\frac{1}{c^2}\int_\Omega\int_0^{2\pi}[N][H][E^T][\rho][H^T[N^T]rd\theta dA\Omega$$
$$[M\rho]=2\pi r_m\frac{1}{c^2}[N][H][E^T][\rho][H^T][N^T]$$
$$[C_r(U_r)]=\frac{1}{c^2}\int_\Omega \psi\,\emptyset^T\rho\psi^T U_r\partial\Omega$$
$$[C_Z(U_Z)]=\frac{1}{c^2}\int_\Omega \psi\,\emptyset^T\rho\psi^T U_Z\frac{\partial\psi^T}{\partial Z}\partial\Omega$$
$$[Q_r]=\frac{1}{Re}\frac{1}{c^2}\int_\Omega\frac{\partial\psi}{\partial r}\emptyset^T\partial\Omega \quad (21)$$
$$[C_r]=\frac{1}{Re}\frac{1}{c^2}\int_\Omega\frac{1}{r}\psi\,\emptyset^T\psi^T U_r\partial\Omega$$
$$[Q_z]=\frac{1}{Re}\frac{1}{c^2}\int_\Omega\frac{\partial\psi}{\partial z}\emptyset^T\partial\Omega \quad (23)$$
$$[C_r(U_r)]=2\pi r_m\frac{1}{c^2}A_{area}[N][H][E][\rho][H^T][N^T][U_r]$$
$$[E^T][B^T][N^T]$$
$$[C_Z(U_Z)]=2\pi r_m\frac{1}{c^2}A_{area}[N][H][E][\rho][H^T][N^T][U_Z]$$
$$[E^T][C^T][N^T]$$
$$[Q]=2\pi r_m\frac{1}{Re}\frac{1}{c^2}A_{area}[N][B][E][E^T]$$
$$[C_r]=2\pi r_m\frac{1}{Re}\frac{1}{c^2}A_{area}[N][H][E^T][\rho][H^T][N^T][U_r]$$

$$[H^T][N^T]$$
$$[Q_Z] = 2\pi r_m \frac{1}{Re}\frac{1}{c^2} A_{area}[N][C][E][E^T]$$

By taking equations 16,17,18 and 19 we can see that a new system of matrix form appeares. As a result, we get the final matrix form of three dimensional unsteady incompressible Navier-Stokes equation based on the artificial compressibility method expressed as:

$$\begin{bmatrix} M\,0\,0\,0\,0 \\ 0\,M\,0\,0\,0 \\ 0\,0\,M\,0\,0 \\ 0\,0\,0\,0\,M_p \end{bmatrix} \begin{bmatrix} \dot{\mu_r} \\ \dot{\mu_\theta} \\ \dot{\mu_z} \\ \rho^{\cdot} \\ \rho^{\cdot} \end{bmatrix} +$$

$$\begin{bmatrix} -C_r(U_r) + C_z(U_z) + \frac{4}{3Re}K_{rr} & C_\theta & \frac{1}{3Re}K_{rz} & -\frac{1}{Re}Q_r & 0 \\ +\frac{4}{3Re}K_r + \frac{4}{3Re}q_r + K_{zz} & & & & \\ 0 & C_r(U_r) + C_z(U_z) + \frac{1}{Re}C_r + \frac{1}{Re}K_{ZZ} & 0 & 0 & 0 \\ & +\frac{1}{Re}K_{rr} + \frac{1}{Re}K_r + \frac{1}{Re}q_\theta & & & \\ -\frac{3}{4Re}K_{rz} + \frac{1}{3Re}K_Z & 0 & C_r(U_r) + C_z(U_z) & -\frac{1}{Re}Q_Z & 0 \\ & \frac{1}{Re}K_{rr} + \frac{1}{Re}K_{Zz} + \frac{1}{Re}K_{rz} + \frac{1}{Re}K_r & & & \\ Q_1 + S & 0 & Q_3 & 0 & 0 \end{bmatrix}$$

$$\begin{bmatrix} \mu_r \\ \mu_\theta \\ \mu_z \\ p \\ \rho \end{bmatrix} = \begin{bmatrix} 0 \\ 0 \\ 0 \\ 0 \\ 0 \end{bmatrix} \qquad (20)$$

.

## 4. Problem discretization

The problem in this article includes the flow of compressible Newtonian fluid selected to be a 2D channel connected to upstream and downstream cylinders. A Poiseuille flow through a 2D-axisymmetric channel is considered in this context, under isothermal conditions. For the numerical porpose, the triangular finite element is applied in this study. In addition, the findings are presented for $\Delta t \approx O(10^{-3})$ and the error criteria are taken as $TOL = 10^{-10}$.

## 5 . Numerical results

The numerical results concerned with the rate of convergence of the problem under consideration by using the Galerkin finite element method based on the artificial compressibility method (AC–method) and the fully artificial compressibility method (FAC–method). The effect of using the artificial compressibility method and fully artificial compressibility method on the convergence rate of pressure for different values of artificial compressibility ($C^2$=5, 100, 500), is illustrated in Figure 1. In both cases, one can see that the level of pressure convergence is decreased as the artificial parameter ($C^2$) increases. Consequently, the profiles reveal that the level of time increments for the AC–method is less than that with FAC–method due to that in AC–method the artificial term is added to the continuity equation only, while this term is added to continuity and momemtum equation simultaneously. For instance, with $C^2$=100 we need around 3100 time-step to get the pressure convergence compared to 12100 time-step for FAC–method; almost (74%) rising. Also, this comparison is very clear for $C^2$=100, where the level of time increments to reach convergence with for FAC–method is five times more than with AC–method (1100 time-step for AC–

method and 5000 time-step for FAC–method), what is found is match with [8,14,15,16].

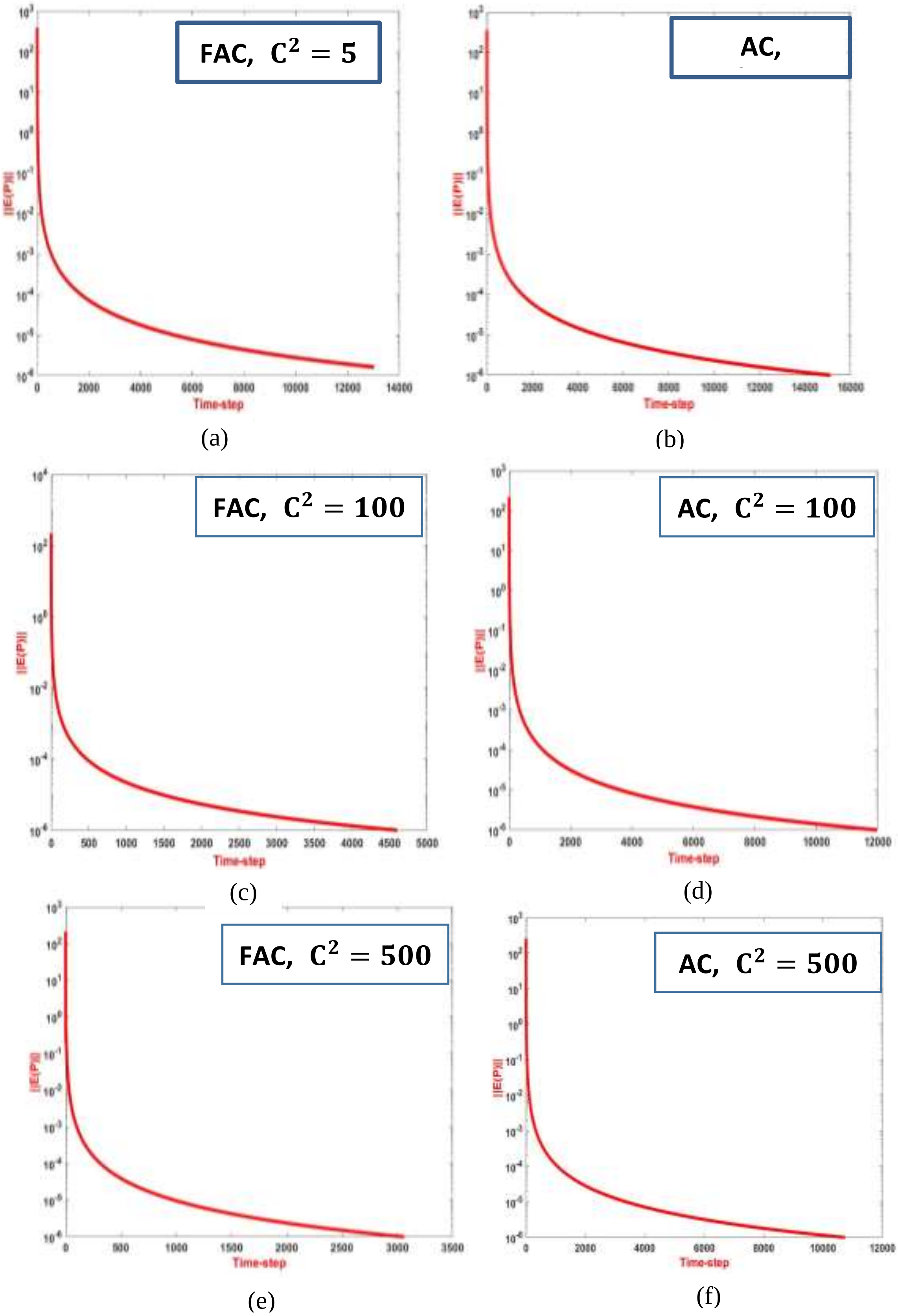


**Figure 1:** Convergence of pressure; $\mathbf{C^2}$-variation, $Re = 1$.

In addition, Figure 2 is provided a similar feature for axial velocity convergence, where the level of time increments decreaeses as the artificial parameter $(C^2)$ rises with a noticeable increase in the case of using the FAC–method because the AC-method gives artificial time, which in turn leads reduce the time that it needs to resolve equations, so it is clear that the values of time steps are less under the artificial compressibility. The level of convergence for the velocity component is high compared to pressure because of the influence of nonlinearity behavior. Thus, we can conclude that the use of AC-method is much easier than FAC-method or direct method [8,14,15,16]. More details are presented in Table1.

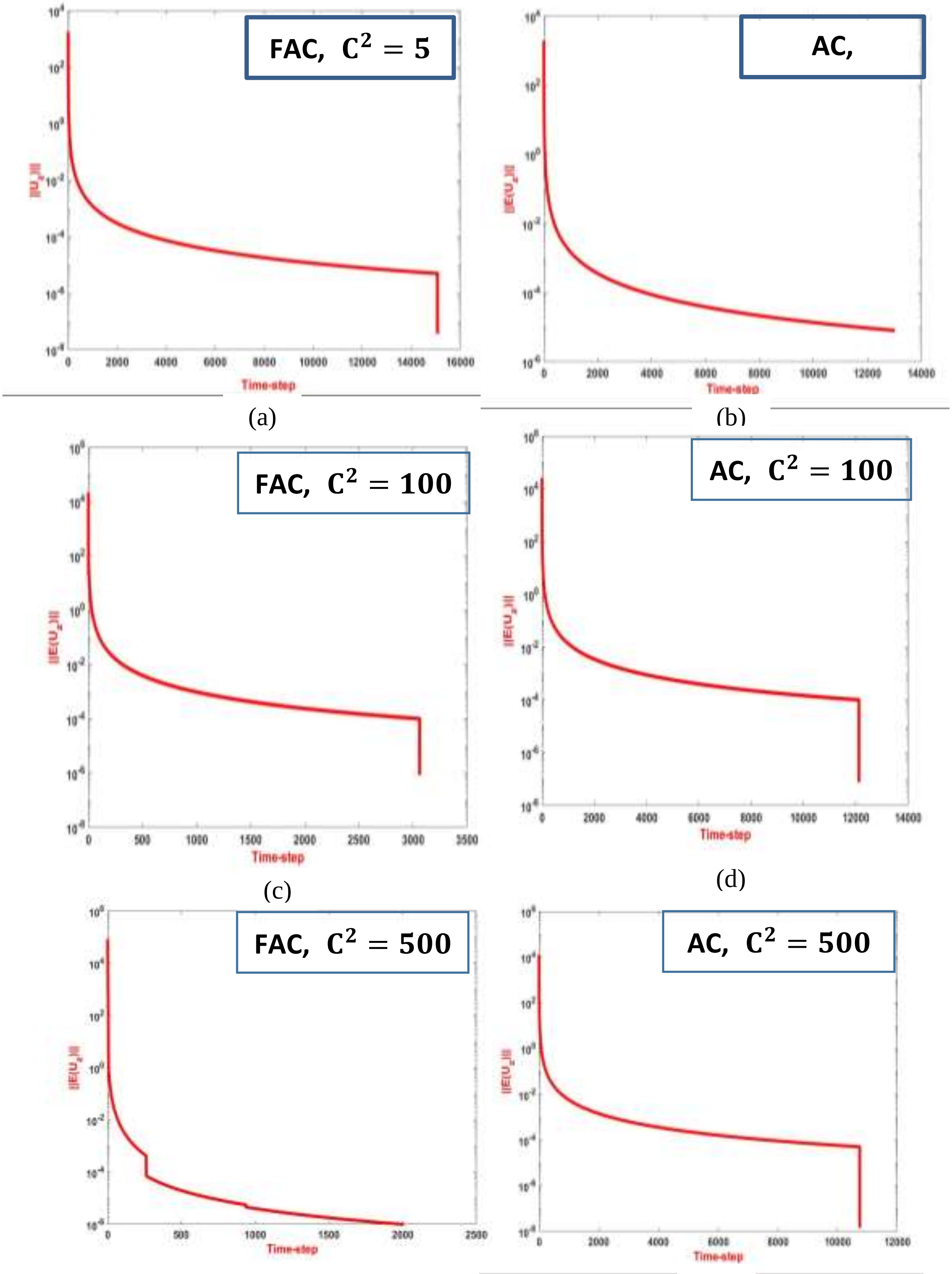


**Figure 2:** Convergence of axial velocity; $\mathbf{C^2}$-variation, $Re = 1$.

**Table 1:** Comparison of error and time; $\mathbf{C^2}$-variation, $Re = 1$.

| | AC-Method | | | | FAC-Method | | | |
|---|---|---|---|---|---|---|---|---|
| $C^2$ | Time-step | Time | $\|p\|_{L_2}$ | $\|u_z\|_{L_2}$ | Time-step | Time | $\|p\|_{L_2}$ | $\|\boldsymbol{u_z}\|_{L_2}$ |
| 5 | 13000 | 13 | $1.34\times10^{-6}$ | $1.80\times10^{-6}$ | 15000 | 15 | $1.57\times10^{-6}$ | $\mathbf{7.8\times10^{-6}}$ |
| 100 | 4600 | 4.6 | $2.77\times10^{-6}$ | $2.41\times10^{-7}$ | 12100 | 12.1 | $1.18\times10^{-5}$ | $\mathbf{1.18\times10^{-5}}$ |
| 500 | 3100 | 3.1 | $3.63\times10^{-6}$ | $2.51\times10^{-7}$ | 11600 | 11.6 | $1.02\times10^{-5}$ | $\mathbf{5.13\times10^{-4}}$ |

## 6. The effect of AC parameters

Here, we describe the results of the effect of Tail parameters variation on the behavior of the solution. In this regard, the focused interest lies in identifying effective of selected parameters {B, m} and *Re* on the level of time stepping convergence and solution components.

**B-effect:** The level of time increments for the AC–method is presented in Figure 3 as a function Tail parameter (m) with different values of Tail Parameter B and Reynolds number Re= {1, 5, 10}. Generally, the results reveal that the level of time-step is decreased as B and m increase, which gives an important indicator of convergence behavior in time. Moreover, as we anticipated, the level of time increments also increased as the level of Re increased. For example, with B=100, Re=1 and m=1 we need around 6200 time-step to get the convergence level compared to 24000 time-step for B=100, Re=10 and m=1; rising by around four times, that because the increase in Reynolds number leads to the velocity gradients will be developed the matter which leads to elongation the time-step, (more detail are also presented in Figure 3).

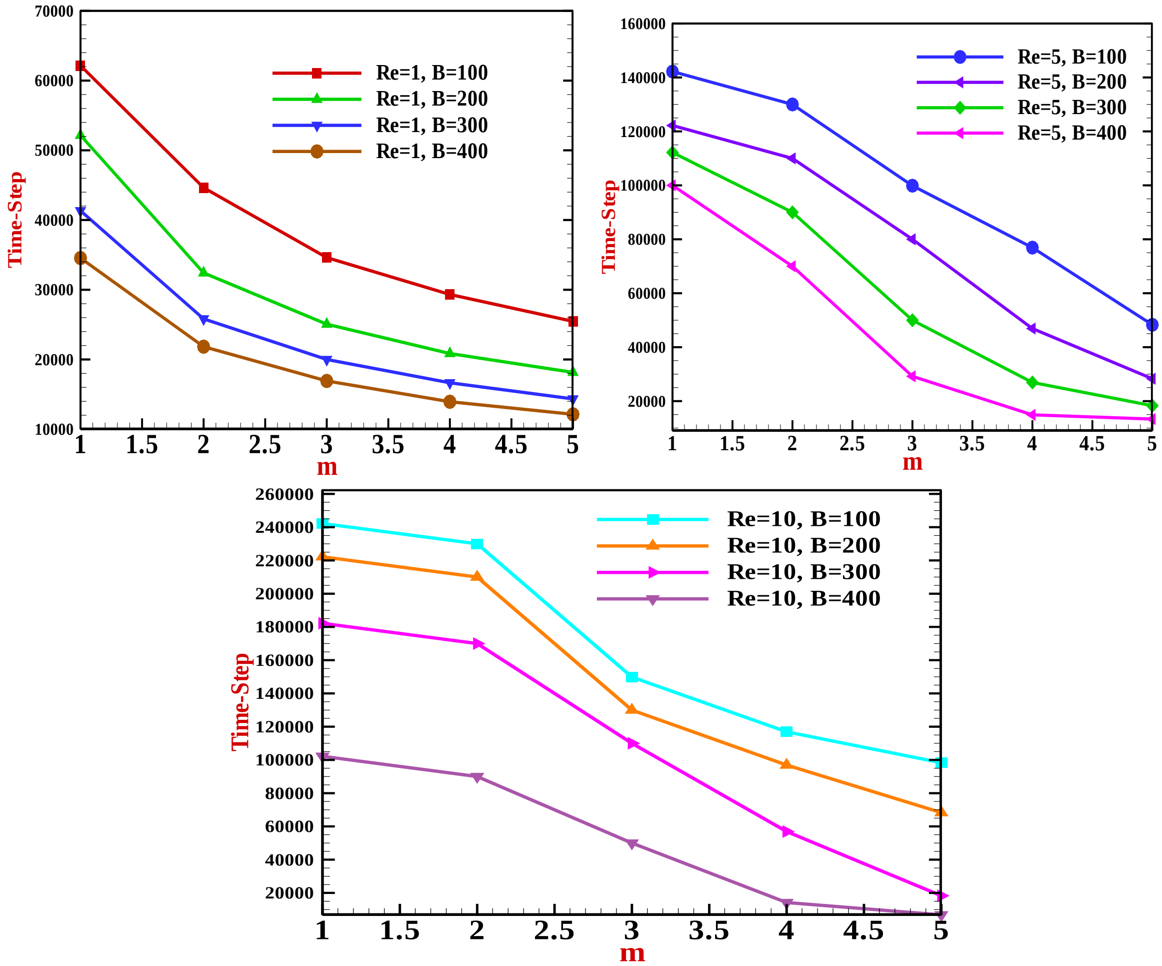


**Figure 3:** Time-step as function of *m* ; B-variation, *Re*=1, 5, 10.

**Re-Effect:** In Figure 4 we show the effect of Reynolds number (*Re*) variation on the behaviors of the solution for B={100, 200, 300, 400} and (1≤m≤5). As anticipated, the profiles provided that, for all values of m the time increments increase as the level of *Re* increases, which reflects the difficulties of the numerical simulation with high level of *Re*. In addition, one can see that the time increments is reduced as the level of B increases because the increase in B value leads to indirect increase in the $C^2$, this reduces the effect of the increase in the value of Re, (see Figure 4b,4c,4d).

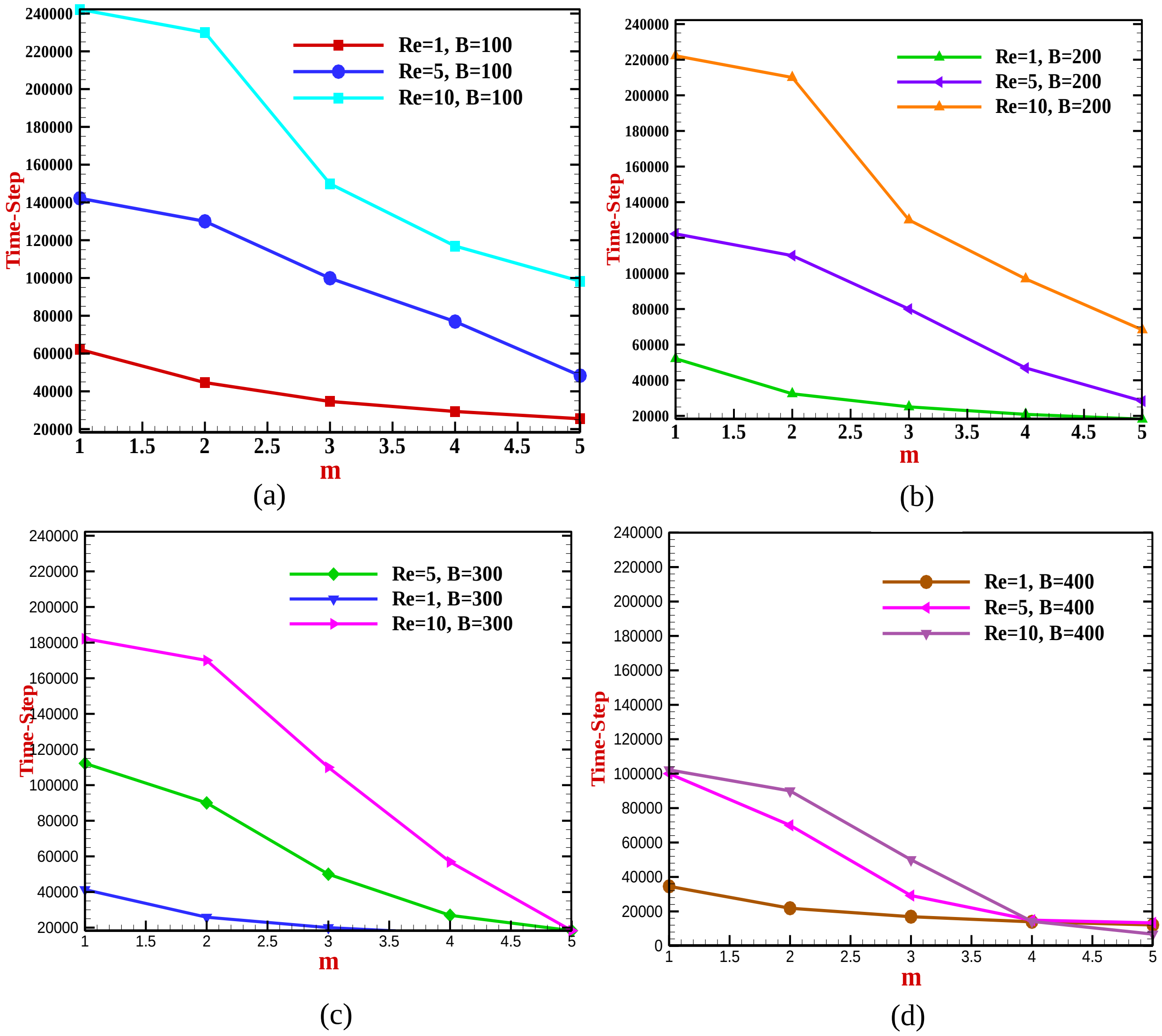


**Figure 4:** Time-step as function of *m* ; *Re*-variation, B=100, 200, 300, 400.

In Figure 5, the axial velocity, pressure drop and density profiles through the centerline are presented for different B-value, m=2 and *Re*=1. The results show that the level of velocity increases as B decreases, reaching to the maximum value of around 2.15 units at the outlet of the channel. Same observations in pressure and density clearly appeared, where the maximum level of pressure of around 16 units and 1.08 units for density are found at the inlet of the channel (see Figure 5b). Table 2 presents more details about the solution components.

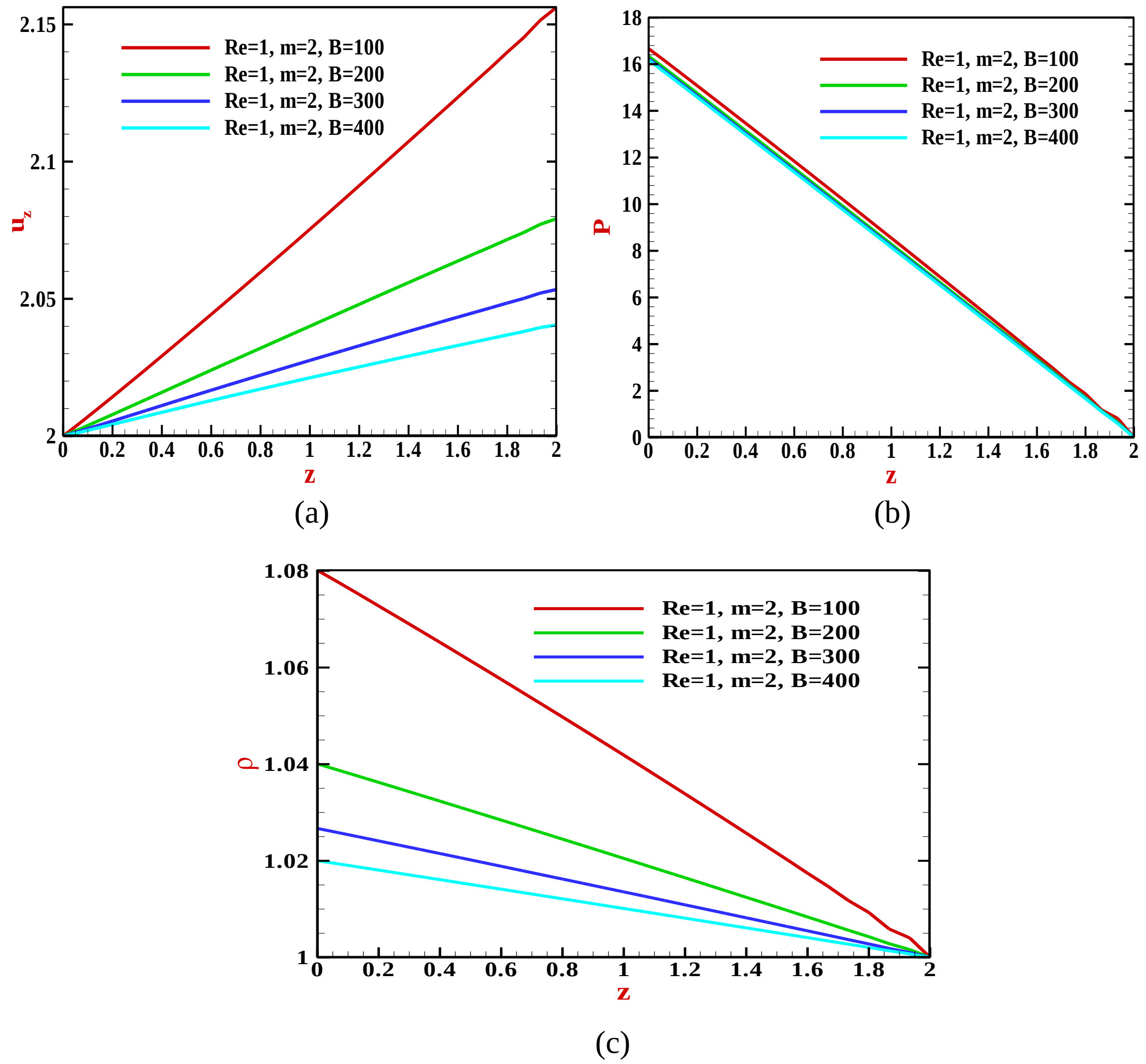


**Figure 5**: Solution components (a) axial velocity, (b) pressure, (c) density; B-variation Re=1, m=2.

**Table 2:** Solution components; B-variation Re=1, m=2.

| M | Max value | B=100 | B=200 | B=300 | B=400 |
|---|---|---|---|---|---|
| m=2 | $u_r$ | 0.0004 | 0.0002 | 0.0001 | 0.0001 |
| | $u_z$ | 2.06 | 2.03 | 2.02 | 2.017 |
| | P | 16.43 | 16.31 | 16.27 | 16.24 |
| | DEN | 1.031 | 1.016 | 1.011 | 1.008 |
| | Mach | 0.092 | 0.064 | 0.052 | 0.045 |
| m=3 | Ur | 0.0007 | 0.0003 | 0.0002 | 0.0001 |
| | Uz | 2.1 | 2.05 | 2.03 | 2.02 |
| | P | 16.61 | 16.41 | 16.33 | 16.29 |
| | DEN | 1.052 | 1.026 | 1.017 | 1.013 |
| | Mach | 0.12 | 0.08 | 0.06 | 0.05 |
| m=4 | Ur | 0.0005 | 0.0002 | 0.0001 | 0.0001 |
| | Uz | 2.07 | 2.04 | 2.02 | 2.02 |
| | P | 16.5 | 16.34 | 16.29 | 16.26 |
| | DEN | 1.03 | 1.019 | 1.013 | 1.01 |
| | Mach | 0.1 | 0.07 | 0.05 | 0.05 |

## 7. Conclusions

In this study, the Galerkin finite element method has been used to simulate compressible and weak-compressible fluid flow based on the artificial compressibility method (AC-mathod) and fully artificial compressibility method (FAC-method). Through the work, we found out that there is a great role of using of AC-method compared to FAC-method in treating compressible and weak compressible fluids, in which convergence of both methods has been assessed. In this context, the convergence rate to steady-state of the AC-method is much better, as compared to that of the FAC-method. In addition,the influence of Tail parameters and *Re* on the acceleration of convergence was done. The findings show that there is a significant effect of these Tail parameters on the time-stepping convergence and the solution, where the level of time convergence is reduced as the Tail parameters rise, such this is an agreement with the findings of others. In contrast, the level of convergence becomes a higher with higher *Re*-value.

## References


**[1]** A. Chorin, "A numerical method for solving incompressible viscous flow problems", *Journal of Computational Physics*, vol. 2, no. 1, pp. 12-26, 1967.

**[2]** J. B.H., S. C., P. P and P. A.K, "Bibliometric Analysis on Artificial Compres- sibility Method based CFD Simulations.", *Library Philosophy and Practice*, 2021.

**[3]** P. Asinari, T. Ohwada, E. Chiavazzo and A. Di Rienzo, "Link-wise artificial compressibility method", *Journal of Computational Physics*, vol. 231, no. 15, pp. 5109-5143, 2012.

**[4]** B. K. Jassim and A. H. Al-Muslimawi, "Numerical analysis of Newtonian flows based on artificial compressibility AC method", *Journal of Al-Qadisiyah for computer science and mathematics*, vol. 9, no. 2, pp. 115-128, 2017.

**[5]** R. Amano and B. Sundén, *Computational fluid dynamics and heat transfer*. Southampton: WIT, 2011.

**[6]** M. Feistauer, J. Felcman and I. Straškraba, *Mathematical and computational methods for compressible flow*. Oxford: Clarendon Press, 2006.

**[7]** P. Kao and R. Yang, "A segregated-implicit scheme for solving the incompressible Navier–Stokes equations", *Computers & Fluids*, vol. 36, no. 6, pp. 1159-1161, 2007.

**[8]** R. Yasir, A. H.Al-Muslimawi and B. K.Jassim, "Numerical simulation of non-Newtonian inelastic flows in channel based on artificial compressibility method", *Journal of Applied and Computational Mechanics*, vol. 6, no. 2, pp. 271-283, 2020.

**[9]** M. Webster, I. Keshtiban and F. Belblidia, "Computation of weakly-compressible highly-viscous liquid flows", *Engineering Computations*, vol. 21, no. 7, pp. 777-804, 2004.

**[10]** M. Khan, T. Salahuddin and Y. Chu, "Analysis of the Carreau fluid model presenting physical properties along different molecular axes near an anisotropic rough surface", *International Communications in Heat and Mass Transfer*, vol. 123, pp. 105233, 2021.

**[11]** E. Tadmor, R. Miller and R. Elliott, *Continuum mechanics and thermodynamics*. Cambridge University Press, 2012.

**[12]** B. Moctar, T. Schellin and H. Soding, *Fundamental Governing Equations. In Numerical Methods for Seakeeping Problems*. Springer, Cham., pp. 5-16, 2021.

**[13]** S. Matsushita and T. Aoki, "Gas-liquid two-phase flows simulation based on weakly compressible scheme with interface-adapted AMR method", *Journal of Computational Physics*, vol. 445, pp. 110605, 2021.

**[14]** M. Rahman and T. Siikonen, "An artificial compressibility method for viscous incompressible and low Mach number flows", *International Journal for Numerical Methods in Engineering*, vol. 75, no. 11, pp. 1320-1340, 2008.

**[15]** M. El Ouafa, S. Vincent and V. Le Chenadec, "Monolithic Solvers for Incompressible Two-Phase Flows at Large Density and Viscosity Ratios", *Fluids*, vol. 6, no.1, pp. 23, 2021.

**[16]** A. Malan, R. Lewis and P. Nithiarasu, "An improved unsteady, unstructured, artificial compressibility, finite volume scheme for viscous incompressible flows: Part I. Theory and implementation", *International Journal for Numerical Methods in Engineering*, vol. 54, no. 5, pp. 695-714, 2002.

**[17]** F. Rouzbahani and K. Hejranfar, "A truly incompressible smoothed particle hydrodynamics based on artificial compressibility method", *Computer Physics Communications*, vol. 210, pp. 10-28, 2017.

**[18]** K. Parseh and K. Hejranfar, "Assessment of Characteristic Boundary Conditions Based on the Artificial Compressibility Method in Generalized Curvilinear Coordinates for Solution of the Euler Equations", *Computational Methods in Applied Mathematics*, vol. 18, no. 4, pp. 717-740, 2017.

**[19]** D. Ntouras and G. Papadakis, "A Coupled Artificial Compressibility Method for Free Surface Flows", *Journal of Marine Science and Engineering*, vol. 8, no. 8, pp. 590, 2020.

**[20]** A. Kajzer and J. Pozorski, "A weakly compressible, diffuse interface model of two-phase flows: Numerical development and validation", *Computers & Mathematics with Applications*, vol. 106, pp. 74-91, 2022.

**[21]** D. Anderson, J. Tannehill and R. Pletcher, *Computational fluid mechanics and heat transfer*. Washington DC: Taylor and Francis, 2016.

**[22]** S. Hosseini and M. Alavianmehr, "New version of Tammann-Tait equation: Application to nanofluids", *Journal of Molecular Liquids*, vol. 220, pp. 404-408, 2016.

**[23]** S. Leloudas, G. Lygidakis, A. Delis and I. Nikolos, "An artificial compressibility method for axisymmetric swirling flows", *Engineering Computations*, vol. 38, no. 10, pp. 3732-3767, 2021.